Hindawi Publishing Corporation
Shock and Vibration
Volume 2014, Article ID 324018, 12 pages
http://dx.doi.org/10.1155/2014/324018

Research Article

Robust Tracking Control for Vehicle Lateral Dynamics with Uncertain Parameters and External Nonlinearities

Huihui Pan, Yifu Zhang, and Weichao Sun

The State Key Laboratory of Robotics and System, Harbin Institute of Technology (HIT), Harbin 150001, China

Correspondence should be addressed to Weichao Sun; 1984sunweichao@gmail.com

Received 16 September 2012; Accepted 12 March 2013; Published 5 March 2014

Academic Editor: Hongyi Li

This paper focuses on the problem of tracking control for vehicle lateral dynamic systems and designs an adaptive robust controller (ARC) based on backstepping technology to improve vehicle handling and stability, in the presence of parameter uncertainties and external nonlinearities. The main target of controller design has two aspects: the first target is to control the sideslip angle as small as possible, and the second one is to keep the real yaw rate tracking the desired yaw rate. In order to compromise the two indexes, the desired sideslip angle is planned as a new reference signal, instead of the ideal "zero." As a result, the designed controller not only accomplishes the control purposes mentioned above, but also effectively attenuates both the changes of vehicle mass and the variations of cornering stiffness. In addition, to overcome the problem of "explosion of complexity" caused by backstepping method in the traditional ARC design, the dynamic surface control (DSC) technique is used to estimate the derivative of the virtual control. Finally, a nonlinear vehicle model is employed as the design example to illustrate the effectiveness of the proposed control laws.

1. Introduction

Because of the large number of traffic accidents occurring daily, vehicle safety control has been a hot research topic. In recent years, vehicle lateral dynamic control has been studied widely for contributing to the car's handling and keeping vehicle ride safe. Especially the yaw-moment control is proved to be an important approach to improve safety performance and has a great potential to meet the requirements demanded by users. To this end, a considerable amount of research has been carried out [1–12], and many vehicle lateral control approaches have been proposed, based on various control techniques, such as fuzzy logic control [13–15], H_∞ control [16], adaptive control [17–20], and nonlinear robust control [21, 22]. Such strategies could considerably enhance vehicle handling and active safety during severe driving maneuvers and, at the same time, allow the driver to keep control of the vehicle when the vehicle is at the physical limit of adhesion between the tires and the road.

In vehicle dynamic systems, inevitable uncertainties often emerge, which will bring considerable difficulties in the process of controller design. For example, because of the change of the number of passengers or the payload, vehicle load is easily varied, which will accordingly change the vehicle mass as a varying parameter. On the other side, the moment of inertia is usually an unknown parameter. Besides, since the yaw-moment control relies on the tire lateral force and the tire force strongly depends on tire vertical load, which is very sensitive to vehicle motion and environmental conditions, the tire cornering stiffness inevitably obtains uncertainties that need to be coped with. Roughly speaking, the abovementioned uncertainties can be classified into two categories: parametric uncertainties (e.g., car body mass for vehicle dynamic control) and general uncertainties (coming from modeling errors and external disturbances). To handle this situation, a number of control techniques have been proposed, such as robust H_∞ or H_2 control [23–26], optimal control [27], fuzzy control [28, 29], sliding mode control [30, 31], neural network control [32–38], adaptive control [39], and fault tolerant control [40, 41]. Besides, during the past decade, a mathematically rigorous nonlinear adaptive robust control theory has also been developed to lay a solid foundation for the design of a new generation of controllers which will help industry build modern machines of great performance and high intelligence [42–44]. This ARC approach can be both adaptive to the

uncertain parameters and at the same time robust against the external disturbances, which is suitable for the systems with uncertainties and the external disturbances, for example, vehicle dynamic systems and robot manipulation systems [45].

The main target of yaw-moment control can be divided into two aspects. The first target is to control the sideslip angle to converge to zero, and the second one is to keep the real yaw rate tracking the desired trajectory. However, these two requirements are conflicting, and it is difficult to achieve both these two indexes simultaneously, especially for the systems with uncertainties. Therefore, a compromise of the requirements must be reached. In this paper, the problem of tracking control for vehicle lateral dynamic systems is investigated, and a backstepping-type adaptive robust controller is designed to improve vehicle handling and stability, in the presence of parameter uncertainties and external nonlinearities. In order to compromise the two tracking indexes, the desired sideslip angle is planned as a new reference signal, instead of the ideal "zero." As a result, the designed controller not only accomplishes the required control purposes, but also effectively attenuates both the changes of vehicle mass and the variations of cornering stiffness. In addition, to overcome the problem of "explosion of complexity" caused by backstepping method in the traditional ARC design, the DSC technique is used to estimate the derivative of the virtual control. Furthermore, the adaptive law is designed to estimate the real value of the moment of inertia. Finally, a nonlinear vehicle model is employed as the design example to illustrate the effectiveness of the proposed control law.

The rest of this paper is organized as follows. The problem to be solved is formulated mathematically in Section 2, and controller design is presented in Section 3, where both the traditional and improved ARC designs are presented. Section 4 provides a design example to illustrate the effectiveness of the proposed control laws and some concluding remarks are given in Section 5.

Nomenclature. The following nomenclature is used throughout the paper: $\widehat{\bullet}$ is used to denote the estimate of $\bullet$, $\widetilde{\bullet}$ is used to denote the parameter estimation error of $\bullet$, and $\bullet_{\max}$, $\bullet_{\min}$ are the maximum and minimum values of $\bullet(t)$ for all t, respectively.

2. Problem Formulation

In this paper, a "bicycle model" is used to model the dynamics of the car, as shown in Figure 1. In this figure, m represents the car chassis; I_z is the moment of inertia about the yaw axis through the center of gravity (CG). The front and rear axles are located at distances l_f and l_r, respectively, from the vehicle CG. The front and rear lateral tire forces F_{yf} and F_{yr} depend on slip angles α_f and α_r, respectively, and the steering angle δ changes the heading of the front tires. β and r stand for the sideslip angle and yaw rate, respectively, and M_z is the external yaw moment. In this paper, it is assumed that the vehicle velocity v is a constant and the steering angle is small.

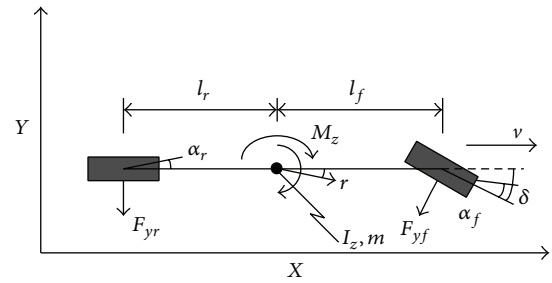

Figure 1: Simplified vehicle "bicycle model."

The equations of the vehicle's handling dynamics in the yaw plane are given as

$$\begin{aligned} mv\dot{\beta}(t) &= F_{yf} + F_{yr} - mvr(t), \\ I_z\dot{r}(t) &= l_f F_{yf} - l_r F_{yr} + M_z(t). \end{aligned} \tag{1}$$

The front and rear lateral tire forces in (1) can be given as

$$\begin{aligned} F_{yf} &= F_{yf0} + f_1(t), \\ F_{yr} &= F_{yr0} + f_2(t), \end{aligned} \tag{2}$$

where

$$F_{yf0} = c_{\alpha f}\alpha_f(t), \qquad F_{yr0} = c_{ar}\alpha_r(t) \tag{3}$$

are the lateral forces at the front and rear wheels in case that the tires operate in the linear region and $f_1(t)$, $f_2(t)$ are the additional nonlinear terms and are bounded. $c_{\alpha f}$ and c_{ar} are the cornering stiffness for the front and rear tires, respectively, and the front and rear slip angles are defined as

$$\begin{aligned} \alpha_f(t) &= \delta(t) - \frac{l_f r(t)}{v} - \beta(t), \\ \alpha_r(t) &= \frac{l_r r(t)}{v} - \beta(t). \end{aligned} \tag{4}$$

Define the nonlinear disturbance uncertainty $\Delta_1(t) = ((f_1(t) + f_2(t))/mv) + w_1(t)$, where w_1 is used to describe the varying of the vehicle mass m. Similarly, we define $\Delta_2(t) = (l_f f_1 - l_r f_2)/I_z$, and it is assumed that $\Delta_i(t) \le d_i(t)$ and $|d_i(t)| \le d_{i\infty}$, $i = 1, 2$, where $d_{i\infty}$ is a positive constant and I_z is the uncertain parameter which satisfies $I_{z\min} \le I_z \le I_{z\max}$. Based on the above definitions, we can rewrite the dynamic equations in (1) as

$$\begin{aligned} \dot{\beta}(t) &= a_1\beta(t) + b_1 r(t) + c_1\delta(t) + \Delta_1(t), \\ \dot{r}(t) &= \theta\left(a_2\beta(t) + b_2 r(t) + c_2\delta(t) + u(t)\right) + \Delta_2(t), \end{aligned} \tag{5}$$

where

$$a_1 = -\frac{\left(c_{\alpha f} + c_{\alpha r}\right)}{mv}, \qquad b_1 = -1 - \frac{l_f c_{\alpha f} - l_r c_{\alpha r}}{mv^2},$$
$$c_1 = \frac{c_{\alpha f}}{mv}, \qquad a_2 = l_r c_{\alpha r} - l_f c_{\alpha f}, \tag{6}$$
$$b_2 = -\frac{\left(l_f^2 c_{\alpha f} + l_r^2 c_{\alpha r}\right)}{v}, \qquad c_2 = l_f c_{\alpha f},$$

and $\theta = 1/I_z \in [\theta_{\min} \quad \theta_{\max}]$ with $\theta_{\min} = 1/I_{z\max}$, $\theta_{\max} = 1/I_{z\min}$ being the uncertain parameter.

Problem 1. For the lateral dynamics systems in (1), synthesize a control input u to control the sideslip angle as small as possible, and keep the real yaw rate tracking the desired trajectory, in the presence of parametric uncertainties and external disturbances.

3. Control Law Synthesis

3.1. Adaptive Robust Controller Design. In this section, an adaptive robust controller is presented to track the desired trajectories of the lateral dynamic systems with uncertain parameters and external disturbances, and the detailed process of controller design is given as follows.

Step 1. Choose $r(t)$ as the virtual control and design a desired function $\alpha(t)$, such that if $r(t) = \alpha(t)$, then the tracking error $e_1 = \beta - \beta_d$ is guaranteed to converge to zero or be bounded, where β_d is the reference trajectory.

Starting with the equation of tracking error, we have

$$\dot{e}_1 = \dot{\beta} - \dot{\beta}_d. \tag{7}$$

Let e_2 be an error variable representing the difference between the actual and virtual control of (7); that is, $e_2 = r - \alpha$. Thus we can rewrite (7) as

$$\dot{e}_1 = a_1\beta + b_1\left(e_2 + \alpha\right) + c_1\delta + \Delta_1 - \dot{\beta}_d. \tag{8}$$

Then, the desired virtual control α can be proposed as

$$\alpha = \alpha_m + \alpha_f + \alpha_s, \tag{9}$$

where

$$\alpha_m = \frac{1}{b_1}\left(\dot{\beta}_d - a_1\beta - c_1\delta\right) \tag{10}$$

is used to achieve a model compensation,

$$\alpha_f = -\frac{k_1}{b_1}e_1 \tag{11}$$

is the stabilizing feedback term, k_1 is a positive design parameter, and α_s is a robust control law designed to satisfy the following conditions:

$$\begin{aligned} &\text{Condition 1: } e_1\left[b_1\alpha_s + \Delta_1\right] \le \varepsilon_1, \\ &\text{Condition 2: } e_1 b_1 \alpha_s \le 0, \end{aligned} \tag{12}$$

where ε_1 is a design parameter which can be arbitrarily small. Basically, condition 1 of (12) shows that α_s is synthesized to dominate the model uncertainties coming from uncertain nonlinearity Δ_1, and condition 2 is to make sure that α_s is dissipating in nature so that it does not interfere with nominal process of control part α_m and α_f. Then, the robust control part α_s can be chosen as

$$\alpha_s = -k_{s1}e_1, \tag{13}$$

where $k_{s1} = d_{1\infty}^2/4b_1\varepsilon_1$. Then, we will show how α_s in (13) guarantees conditions 1 and 2 in (12).

Substituting α_s into condition 1 in (12), we have

$$\begin{aligned} &e_1\left(b_1\alpha_s + \Delta_1\right) \\ &\quad \le -\frac{d_{1\infty}^2}{4\varepsilon_1}e_1^2 + |e_1|\,|d_{1\infty}| \\ &\quad \le -\left[\left(\frac{|e_1|\,|d_{1\infty}|}{2\sqrt{\varepsilon_1}}\right)^2 - |e_1|\,|d_{1\infty}| + \left(\sqrt{\varepsilon_1}\right)^2\right] + \varepsilon_1 \le \varepsilon_1. \end{aligned} \tag{14}$$

Substituting (9)–(11) and (13) into (8) results in

$$\dot{e}_1 = b_1 e_2 - k_1 e_1 + b_1\alpha_s + \Delta_1. \tag{15}$$

Step 2. Synthesize an adaptive robust control law for u, so that the error e_2 is bounded in the presence of uncertain parameter θ and external disturbances Δ_i, $i = 1, 2$.

Differentiating the error dynamics for $e_2 = r - \alpha$ results in

$$\dot{e}_2 = \theta\varphi(t) + \Delta_2 - \dot{\alpha}, \tag{16}$$

where $\varphi(t) = a_2\beta + b_2 r + c_2\delta + u$. Design the control input

$$u = u_a + u_s, \tag{17}$$

$$u_a = -a_2\beta - b_2 r - c_2\delta + \frac{1}{\widehat{\theta}}\left(-k_2 e_2 - b_1 e_1 + \dot{\alpha}'\right), \tag{18}$$

$$u_s = -k_{s2}e_2, \tag{19}$$

where k_2 is a positive design parameter and $\dot{\alpha}'$, $\dot{\alpha}''$ respect the certain and uncertain parts of $\dot{\alpha}u_s = -k_{s2}e_2$ is a robust control law designed to satisfy the following conditions:

$$\begin{aligned} &\text{Condition 1: } e_2\left(\widehat{\theta}u_s - \widetilde{\theta}\varphi(t) + \Delta_2 - \dot{\alpha}''\right) \le \varepsilon_2, \\ &\text{Condition 2: } e_2\widehat{\theta}u_s \le 0, \end{aligned} \tag{20}$$

where ε_2 is a design parameter which can be arbitrarily small. To satisfy the conditions above, one can choose the nonlinear control gain k_{s2} as

$$k_{s2} = \frac{h_2^2(t)}{4\theta_{\min}\varepsilon_2}, \tag{21}$$

where $h_2(t)$ is a function which satisfies

$$\widetilde{\theta}\varphi(t) + \Delta_2 - \dot{\alpha}'' \le \left|\theta_{\max} - \theta_{\min}\right| \left|\varphi(t)\right| + d_{2\infty} + \left|\dot{\alpha}''\right| = h_2(t). \tag{22}$$

$\widehat{\theta}$ is the estimation of θ, which is chosen as the projection type with the following form:

$$\dot{\widehat{\theta}} = \mathrm{Proj}_{\widehat{\theta}}\left(r_m^{-1}\tau\right), \tag{23}$$

and $r_m > 0$ is a tunable gain and $\tau = \varphi(t)e_2$. The standard projection mapping $\mathrm{Proj}_{\widehat{\theta}}(r_m^{-1}\tau)$ is introduced as

$$\mathrm{Proj}_{\widehat{\theta}}\left(r_m^{-1}\tau\right) = \begin{cases} 0, & \text{if } \widehat{\theta} = \theta_{\max},\ r_m^{-1}\tau > 0, \\ 0, & \text{if } \widehat{\theta} = \theta_{\min},\ r_m^{-1}\tau < 0, \\ r_m^{-1}\tau, & \text{otherwise.} \end{cases} \tag{24}$$

This projection mapping $\mathrm{Proj}_{\widehat{\theta}_1}(r\tau)$ guarantees that the parameter estimate is always within the known bounds, that is, $\theta_{\min} < \theta < \theta_{\max}$, and $\widetilde{\theta}(r_m^{-1}\mathrm{Proj}_{\widehat{\theta}}(r\tau) - \tau) \le 0$, for all τ, which enables one to show that the use of projection modification to the traditional integral type adaptation law does not interfere with the perfect learning capability of the original integral type adaptation law.

Then, substituting (17)–(23) into (16) results in

$$\begin{aligned} \dot{e}_2 &= \widehat{\theta}\left(a_2\beta + b_2 r + c_2\delta + u\right) - \widetilde{\theta}\varphi(t) + \Delta_2 - \dot{\alpha} \\ &= -k_2 e_2 - b_1 e_1 + \dot{\alpha}' + \widehat{\theta}u_s - \widetilde{\theta}\varphi(t) + \Delta_2 - \dot{\alpha} \\ &= -k_2 e_2 - b_1 e_1 + \widehat{\theta}u_s - \widetilde{\theta}\varphi(t) + \Delta_2 - \dot{\alpha}''. \end{aligned} \tag{25}$$

The structure diagram of the adaptive robust controller design is given in Figure 2, and based on the above processing of controller design, we have the following theorem.

Theorem 2. *If u is designed as* (17)–(19)*, and the adaptive law is chosen as* (23)*, then the following results hold.*

(a) *In general (i.e., the system is subjected to parametric uncertainties, unmodelled uncertainties, and external disturbances), both the tracking errors e_1 and e_2 are bounded and, specifically, defining $\lambda_0 = \min(k_1, k_2)$, the steady-state output tracking errors e_1 and e_2 are bounded by $|e_1(\infty)| \le \sqrt{(\varepsilon_1 + \varepsilon_2)/\lambda_0}$, $|e_2(\infty)| \le \sqrt{(\varepsilon_1 + \varepsilon_2)/\lambda_0}$.*

(b) *If, after a finite time, the system is subjected to parametric uncertainties only (i.e., all the disturbances vanish after a finite time), both the tracking errors e_1 and e_2 will asymptotically converge to zero.*

Proof. Firstly, the proof of statement (a) is given. Choose a positive definite function as

$$V = \frac{1}{2}e_1^2 + \frac{1}{2}e_2^2, \tag{26}$$

whose derivative is given as

$$\begin{aligned} \dot{V} &= e_1\dot{e}_1 + e_2\dot{e}_2 \\ &= e_1\left(b_1 e_2 - k_1 e_1 + b_1\alpha_s + \Delta_1\right) \\ &\quad + e_2\left(-k_2 e_2 - b_1 e_1 + \widehat{\theta}u_s - \widetilde{\theta}\varphi(t) + \Delta_2 - \dot{\alpha}''\right) \\ &= -k_1 e_1^2 - k_2 e_2^2 + e_1\left(b_1\alpha_s + \Delta_1\right) \\ &\quad + e_2\left(\widehat{\theta}u_s - \widetilde{\theta}\varphi(t) + \Delta_2 - \dot{\alpha}''\right) \\ &\le -k_1 e_1^2 - k_2 e_2^2 + \varepsilon_1 + \varepsilon_2. \end{aligned} \tag{27}$$

After defining λ_0, we have

$$\dot{V} \le -2\lambda_0 V + \varepsilon_1 + \varepsilon_2, \tag{28}$$

which can further result in

$$V(t) \le \frac{\varepsilon_1 + \varepsilon_2}{2\lambda_0} + \left(V(0) - \frac{\varepsilon_1 + \varepsilon_2}{2\lambda_0}\right)e^{-2\lambda_0 t}. \tag{29}$$

Inequality (29) implies that $V(\infty) \le (\varepsilon_1 + \varepsilon_2)/2\lambda_0$, which guarantees

$$\left|e_1(\infty)\right| \le \sqrt{\frac{\varepsilon_1 + \varepsilon_2}{\lambda_0}}, \qquad \left|e_2(\infty)\right| \le \sqrt{\frac{\varepsilon_1 + \varepsilon_2}{\lambda_0}}. \tag{30}$$

Therefore, the proof of statement (a) is completed.

If, after a finite time, the system is only subjected to parametric uncertainties, the dynamic systems can be written as

$$\begin{aligned} \dot{\beta}(t) &= a_1\beta(t) + b_1 r(t) + c_1\delta(t), \\ \dot{r}(t) &= \theta\left(a_2\beta(t) + b_2 r(t) + c_2\delta(t) + u(t)\right). \end{aligned} \tag{31}$$

Choose a positive definite function as

$$V_\theta = \frac{1}{2}e_1^2 + \frac{1}{2}e_2^2 + \frac{1}{2}r_m\widetilde{\theta}^2, \tag{32}$$

and then we have

$$\begin{aligned} \dot{V}_\theta &= e_1\dot{e}_1 + e_2\dot{e}_2 + r_m\widetilde{\theta}\dot{\widehat{\theta}} \\ &\le -k_1 e_1^2 - k_2 e_2^2 + \widetilde{\theta}\left(r_m\dot{\widehat{\theta}} - \varphi(t)e_2\right). \end{aligned} \tag{33}$$

Noticing the property of the projection mapping

$$\mathrm{Proj}_{\widehat{\theta}}\left(r_m^{-1}\tau\right): \widetilde{\theta}\left(r_m\mathrm{Proj}_{\widehat{\theta}}\left(r_m^{-1}\tau\right) - \tau\right) \le 0, \quad \forall\tau, \tag{34}$$

we have

$$\dot{V}_\theta \le -k_1 e_1^2 - k_2 e_2^2 \le 0. \tag{35}$$

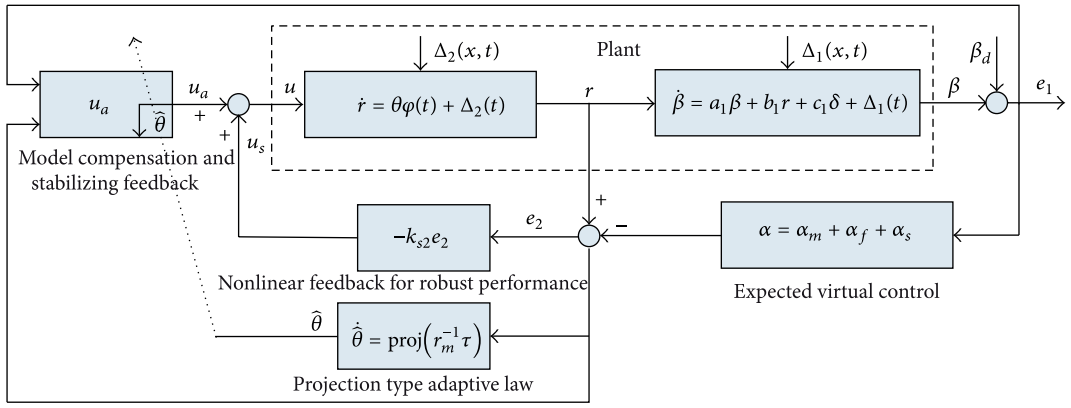

Figure 2: Structure diagram of the adaptive robust controller design.

Integrating both sides of inequality $\dot{V}_\theta \le 0$ from 0 to t results in

$$V_\theta(t) = \int_0^t \dot{V}_\theta d\tau + V_\theta(0) \le V_\theta(0), \tag{36}$$

which implies $e_1, e_2, \widetilde{\theta} \in L_\infty$, and thus $\beta, \alpha, r \in L_\infty$. Therefore,

$$\dot{e}_1, \dot{e}_2 \in L_\infty, \tag{37}$$

and thus

$$\begin{aligned} &\ddot{V}_\theta \le -2k_1 e_1 \dot{e}_1 - 2k_2 e_2 \dot{e}_2 \in L_\infty \\ &\quad \Longrightarrow \dot{V}_\theta \text{ is uniformly continuous.} \end{aligned} \tag{38}$$

By using Lyapunov-like lemma, we have $\dot{V}_\theta \to 0$ as $t \to \infty$, which means that the tracking errors e_1 and e_2 converge to zero asymptotically. The proof is completed. □

Remark 3. As stated above, our main target has two aspects: the first target is to control the sideslip angle to converge to zero, and the second one is to keep the real yaw rate tracking the desired trajectory. However, these two requirements are conflicting, and it is difficult to achieve both these two indexes simultaneously, especially for the systems with uncertainties and nonlinearities. Therefore, a compromise of the requirements must be reached. To handle this situation, in this paper, the desired sideslip angle is replanned as follows:

$$\beta_d(s) = \frac{1}{s^2 + k_{w1}s + k_{w2}}\text{ref}(s), \tag{39}$$

where

$$\begin{aligned} k_{w1} &= k_1 + k_z + \frac{d_{1\infty}^2}{4\varepsilon_1}, \\ k_{w2} &= k_z\left(k_1 + \frac{d_{1\infty}^2}{4\varepsilon_1}\right), \\ \text{ref}(t) &= \left(a_1 + k_1 + \frac{d_{1\infty}^2}{4\varepsilon_1}\right)\dot{\beta} + (c_1 + b_1 q)\dot{\delta} - b_1 k_z z_d, \\ z_d &= \frac{1}{b_1}\left(-\left(a_1 + k_1 + \frac{d_{1\infty}^2}{4\varepsilon_1}\right)\beta - c_1\delta\right) - q\delta, \end{aligned} \tag{40}$$

and k_z is a positive constant. Using this trajectory in (39) to replace the desired trajectory zero, we can guarantee that the virtual input α converges to the desired yaw rate $r_d = q\delta$, where

$$q = \frac{v}{\left(l_f + l_r\right)\left(1 + k_{us}v^2\right)}\delta(t), \tag{41}$$

in which k_{us} is a stability factor.

Next, we will give the proof that α will converge to the desired yaw rate r_d, using the designed β_d. Defining

$$z = \alpha - r_d \tag{42}$$

and choosing a positive function as

$$V_\beta = \frac{1}{2}z^2, \tag{43}$$

we have

$$\begin{aligned} \dot{V}_\beta &= z\left(\dot{\alpha} - \dot{r}_d\right) \\ &= z\left(\frac{1}{b_1}\left(\ddot{\beta}_d - a_1\dot{\beta} - c_1\dot{\delta} - \left(k_1 + \frac{d_{1\infty}^2}{4\varepsilon_1}\right)\dot{e}_1\right) - q\dot{\delta}\right). \end{aligned} \tag{44}$$

Substituting (39) into (44) results in

$$\dot{V}_\beta = -k_z z^2 \le 0, \tag{45}$$

which means that z will converge to zero as $t \to \infty$, and it further implies that α coverages to the desired yaw rate r_d.

Remark 4. Actuator saturation appears frequently in engineering systems, which is also a source of performance degradation and the closed-loop system instability. Roughly speaking, all actuators of physical devices are subject to amplitude saturation. Although, in some applications, it may be possible to ignore this fact, the reliable operation and acceptable performance of most control systems must be assessed in light of actuator saturation. From the analysis above, it is known that all the signals are bounded within the known ranges, and thus the actuator saturation constraints will be guaranteed as long as the initial values and tuning gains $(k_1, k_2, k_{s1}, k_{s2})$ are adjusted properly.

3.2. Adaptive Robust Controller Design via DSC Technique. From the design process above, it can been seen that it is quite complicated to obtain $\dot{\alpha}$, especially to split $\dot{\alpha}$ into the known part $\dot{\alpha}'$ and the unknown part $\dot{\alpha}''$. To overcome the problem of "explosion of complexity" caused by backstepping method in the traditional ARC design, the dynamic surface control technique is used to estimate the derivative of the virtual control $\dot{\alpha}$. Therefore, the design process for Step 2 is modified as follows.

Modified Step 2. Let α pass through a first-order filter with time constant τ_2, which means

$$\tau_2 \dot{\overline{\alpha}} + \overline{\alpha} = \alpha, \quad \overline{\alpha}(0) = \alpha(0). \tag{46}$$

Defining the estimate errors as $y_2 = \overline{\alpha} - \alpha$, $e_2 = r - \overline{\alpha}$, the derivative of e_1 can be rewritten as

$$\dot{e}_1 = b_1 e_2 - k_1 e_1 + b_1 \alpha_s + b_1 y_2 + \Delta_1. \tag{47}$$

Differentiating the error dynamics for $e_2 = r - \overline{\alpha}$ results in

$$\dot{e}_2 = \theta \varphi(t) + \Delta_2 + \frac{y_2}{\tau_2}. \tag{48}$$

After choosing the adaptive robust controller u as

$$\begin{aligned} u &= u_a + u_s, \\ u_a &= -a_2\beta - b_2 r - c_2\delta + \frac{1}{\widehat{\theta}}\left(-k_2 e_2 - b_1 e_1 - \frac{y_2}{\tau_2}\right), \\ u_s &= -k_{2s} e_2, \end{aligned} \tag{49}$$

we can obtain the error dynamic systems as

$$\begin{aligned} \dot{e}_1 &= b_1 e_2 - k_1 e_1 + b_1 \alpha_s + b_1 y_2 + \Delta_1, \\ \dot{e}_2 &= -b e_1 - k_2 e_2 + \widehat{\theta} u_s - \widetilde{\theta}\varphi(t) + \Delta_2, \\ \dot{y}_2 &= -\frac{y_2}{\tau_2} - \dot{\alpha}, \end{aligned} \tag{50}$$

where $u_s = -k_{2s} e_2$ is a robust control law designed to satisfy the following conditions:

$$\begin{aligned} &\text{Condition 1: } e_2\left(\widehat{\theta} u_s - \widetilde{\theta}\varphi(t) + \Delta_2\right) \le \varepsilon_{2s}, \\ &\text{Condition 2: } e_2 \widehat{\theta} u_s \le 0, \end{aligned} \tag{51}$$

where ε_{2s} is a design parameter which can be arbitrarily small. Similarly, we can choose the nonlinear control gain k_{2s} as $k_{2s} = (h_3^2(t)/4\theta_{\min}\varepsilon_{2s})$, where $h_3(t)$ is a function which satisfies

$$\widetilde{\theta}\varphi(t) + \Delta_2 \le \left|\theta_{\max} - \theta_{\min}\right| \left|\varphi(t)\right| + d_{2\infty} = h_3(t). \tag{52}$$

Furthermore, since all terms in $\dot{\alpha}$ can be dominated by some continuous functions $B_2(e_1, e_2, y_2, \widehat{\theta}, \beta_d, \dot{\beta}_d)$, we have

$$\left|\dot{y}_2 + \frac{y_2}{\tau_2}\right| \le B_2\left(e_1, e_2, , y_2 \widehat{\theta}, \beta_d, \dot{\beta}_d\right), \tag{53}$$

which implies

$$y_2 \dot{y}_2 \le -\frac{y_2^2}{\tau_2} + B_2\left|y_2\right| \le -\frac{y_2^2}{\tau_2} + y_2^2 + \frac{1}{4}B_2^2. \tag{54}$$

Before the main result is given, the following definitions are given. For any $p > 0$, define

$$\Pi = \left\{\left(e_1, e_2, y_2, \widehat{\theta}\right) : V_d(t) \le p\right\}, \tag{55}$$

where

$$V_d(t) = \frac{1}{2}e_1^2 + \frac{1}{2}e_2^2 + \frac{1}{2}y_2^2 + \frac{1}{2r_m}\widetilde{\theta}^2. \tag{56}$$

Obviously, Π is a compact subset; hence there must be a point corresponding to the supreme value of B_2 in Π. We denote this supreme value as M_2; that is,

$$B_2 \le M_2. \tag{57}$$

Theorem 5. *If the virtual input, control input, and adaptive law are designed as* (9), (49), *and* (23), *respectively, then, for any initial states in* Π, *there exist positive parameters* $k_1, k_{2s}, \tau_2, r_m, \varepsilon_1$, *and* ε_{2s} *satisfying*

$$\begin{aligned} k_1 - \frac{b_1}{2} &\ge \rho, \\ k_2 &\ge \rho, \\ \frac{1}{\tau_2} - 1 - \frac{b_1}{2} &\ge \rho, \\ \rho &> 0, \end{aligned} \tag{58}$$

such that the tracking errors e_1, e_2, *and* y_2 *are uniformly ultimately bounded and the steady-state tracking error can be made arbitrarily small.*

Proof. Define a positive function as shown in (56). The derivative of $V_d(t)$ is

$$\begin{aligned}\dot{V}_d(t) &= e_1\dot{e}_1 + e_2\dot{e}_2 + y_2\dot{y}_2 + r_m^{-1}\tilde{\theta}\dot{\tilde{\theta}} \\ &= e_1\left(b_1e_2 - k_1e_1 + b_1y_2 + b_1\alpha_s + \Delta_1\right) + y_2\dot{y}_2 \\ &\quad + r_m^{-1}\tilde{\theta}\dot{\tilde{\theta}} + e_2\left(-be_1 - k_2e_2 + \hat{\theta}u_s - \tilde{\theta}\varphi(t) + \Delta_2\right).\end{aligned} \tag{59}$$

Noting that

$$b_1e_1y_2 \le \frac{b_1}{2}\left(e_1^2 + y_2^2\right), \tag{60}$$

we have

$$\begin{aligned}\dot{V}_d(t) \le &-\left(k_1 - \frac{b_1}{2}\right)e_1^2 - k_2e_2^2 - \left(\frac{1}{\tau_2} - 1 - \frac{b_1}{2}\right)y_2^2 \\ &- r_m^{-1}\rho\tilde{\theta}^2 + \varepsilon_1 + \varepsilon_{2s} + \frac{1}{4}M_2^2 + r_m^{-1}\rho\tilde{\theta}^2.\end{aligned} \tag{61}$$

Based on conditions (58), we have

$$\dot{V}_d(t) \le -2\rho V_d(t) + R_0, \tag{62}$$

where $R_0 = \varepsilon_1 + \varepsilon_{2s} + (1/4)M_2^2 + \rho M_\theta$ with $M_\theta = r_m^{-1}(\theta_{\max} - \theta_{\min})^2$. Inequality (62) can further result in

$$V_d(t) \le \frac{R_0}{2\rho} + \left(V_d(0) - \frac{R_0}{2\rho}\right)e^{-2\rho t}, \tag{63}$$

which implies that e_1, e_2, and y_2 are bounded as

$$\begin{aligned}&|e_1(\infty)| \le \sqrt{\frac{R_0}{\rho}}, \qquad |e_2(\infty)| \le \sqrt{\frac{R_0}{\rho}}, \\ &|y_2(\infty)| \le \sqrt{\frac{R_0}{\rho}}.\end{aligned} \tag{64}$$

Next, we will show that the steady-state tracking errors e_1, e_2, and y_2 can be made arbitrarily small. Define a positive definite function $\overline{V}_d(t)$ satisfying

$$\overline{V}_d(t) = \frac{1}{2}e_1^2 + \frac{1}{2}e_2^2 + \frac{1}{2}y_2^2. \tag{65}$$

In order to make a contradiction, we assume that there exists $T > 0$ so that, when $t > T$,

$$\overline{V}_d(t) > \frac{R}{2\rho} + \sigma, \tag{66}$$

where $R = \varepsilon_1 + \varepsilon_{2s} + (1/4)M_2^2$ and σ is a positive constant which can be set arbitrarily small. On the other hand, the following inequality is true:

$$\begin{aligned}\dot{V}_d(t) &\le -2\rho V_d(t) + \varepsilon_1 + \varepsilon_{2s} + \frac{1}{4}M_2^2 + r_m^{-1}\rho\tilde{\theta}^2 \\ &= -2\rho\overline{V}_d(t) - r^{-1}\rho\tilde{\theta}^2 + \varepsilon_1 + \varepsilon_{2s} + \frac{1}{4}M_2^2 + r^{-1}\beta\tilde{\theta}^2 \\ &= -2\rho\overline{V}_d(t) + R.\end{aligned} \tag{67}$$

Table 1: The model parameters of vehicle lateral systems.

Parameter	Value
m	1100–1300 kg
$I_{z\max}$	1700 kgm^2
$c_{\alpha f}$	20000 N/m
l_f	1 m
k_{us}	0.03
I_z	1600 kgm^2
$I_{z\min}$	1500 kgm^2
$c_{\alpha r}$	20000 N/m
l_r	1.5 m
v	20 m/s

Integrating both sides of the above inequality from zero to any $t > 0$, we obtain

$$V_d(t) - V_d(0) \le \int_0^t \left(-2\rho\overline{V}_d(t) + R\right)dt. \tag{68}$$

Because $V_d(t)$ is bounded, we have

$$f(t) = \int_0^t \left(2\rho\overline{V}_d(t) - R\right)dt \le V_d(0) - V_d(t) \tag{69}$$

is bounded as well. It is obvious that

$$\ddot{f}(t) = 2\rho\dot{\overline{V}}_d(t) = 2\rho\left(e_1\dot{e}_1 + e_2\dot{e}_2 + y_2\dot{y}_2\right) \tag{70}$$

is bounded, and then, based on Barbalat's lemma, we have

$$\lim_{t\to\infty}\dot{f}(t) = \lim_{t\to\infty}\left(2\rho\overline{V}_d(t) - R\right) = 0, \tag{71}$$

which implies

$$\overline{V}_d(t) \le \frac{R}{2\rho} + \sigma. \tag{72}$$

Therefore, the tracking errors e_1, e_2, and y_2 are uniformly ultimately bounded and the steady-state tracking error can be made arbitrarily small by properly choosing tuning parameters. □

4. A Design Example

In this section, we provide an example to illustrate the effectiveness of the proposed approach. The vehicle model parameters are listed in Table 1.

The initial state values are assumed as zeros, and $\theta(0) = 1/1500$. The controller parameters are given in Table 2.

For checking the vehicle lateral dynamic performance in terms of the change of vehicle mass, three different masses are tested to illustrate the effectiveness of robust control:

(S1) closed-loop systems with the vehicle mass m = 1100 kg;

(S2) closed-loop systems with the vehicle mass m = 1200 kg;

(S3) closed-loop systems with the vehicle mass m = 1300 kg;

(S4) open-loop systems without controller.

Table 2: The controller parameters of adaptive robust controller.

Parameter	Value
r_m	1000
k_1	10
k_2	10
k_z	10
k_{s1}	10
k_{s2}	10
k_{2s}	10

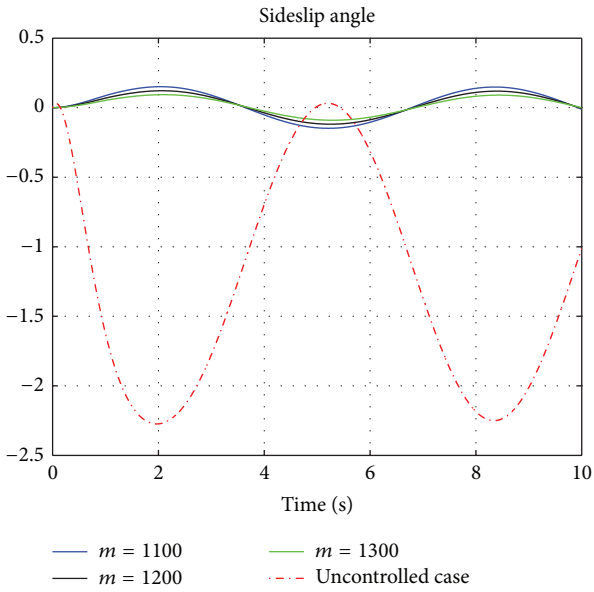

Figure 3: The sideslip angle responses of the open-loop system, closed-loop systems with designed ARC controller for different vehicle masses.

4.1. Periodic Demand Signal. In order to illustrate the effectiveness of the proposed control law, in this paper, it is assumed that the steering angle $\delta = \sin(t)$, and the lumped nonlinearities

$$\Delta_i(t) = \begin{cases} 0.01\sin(t), & 0 \le t \le 1, \\ 0, & \text{otherwise.} \end{cases} \tag{73}$$

The sideslip angle responses of the open-loop system, closed-loop systems with designed ARC controller for different vehicle masses are compared in Figure 3, and Figure 4 is the local enlargement of Figure 3 from −0.5 to 0.5 at y-axis. From these two figures, we can see that the response peak has been reduced substantially, by using the proposed controller, compared with the open-loop system without controller. Also, we can get the conclusion that the sideslip angle performance is still guaranteed at a high level, although there are changing vehicle masses, external disturbances, and other uncertainties.

Figures 5 and 6 show the time histories of yaw rate for both open-loop systems and closed-loop systems with ARC controller in the case of different vehicle masses, and Figures 7 and 8 are the corresponding responses of tracking errors

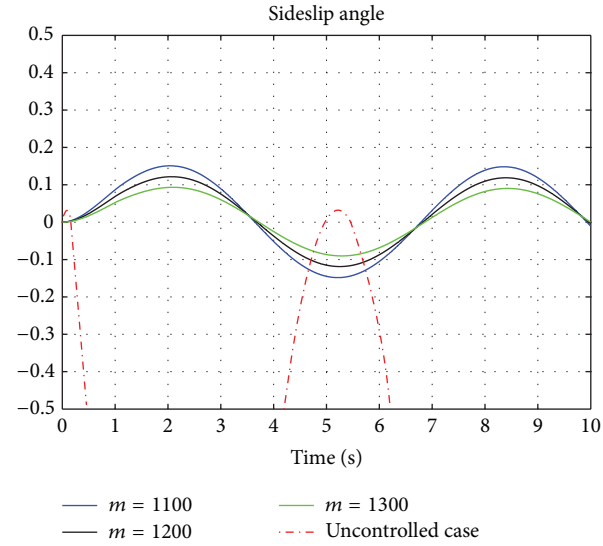

Figure 4: The local enlargement of Figure 3.

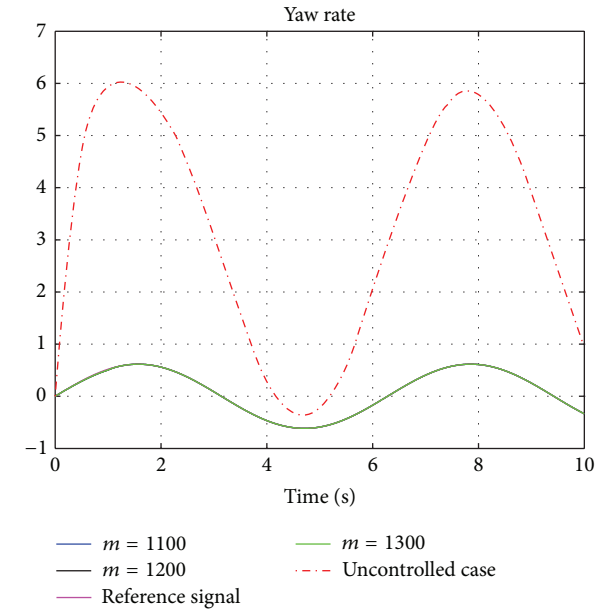

Figure 5: The yaw rate responses of the open-loop system, closed-loop systems with designed ARC controller for different vehicle masses.

between the real yaw rate and the desired yaw rate. It can be seen that the closed-loop systems with the proposed ARC controllers can track the desired trajectories perfectly. By contrast, the open-loop systems without controller cannot do this work, and the tracking errors of the open-loop systems are very large. From Figures 5 and 6, we observe that the yaw rate response of the controlled system is better than the uncontrolled system, regardless of the change of vehicle mass. In particular, from Figures 7 and 8, the tracking errors are close to zero, and the yaw rates are all smaller than the corresponding uncontrolled system responses.

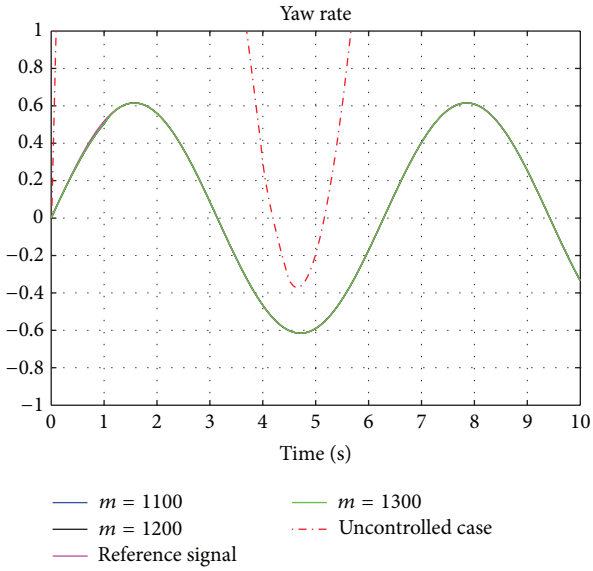

Figure 6: The local enlargement of Figure 5.

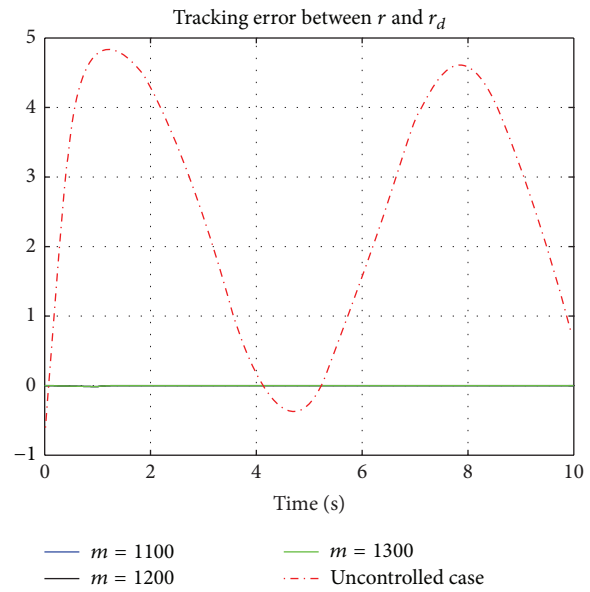

Figure 7: The tracking errors between real yaw rate and desired yaw rate of the open-loop system, closed-loop systems with designed ARC controller for different vehicle masses.

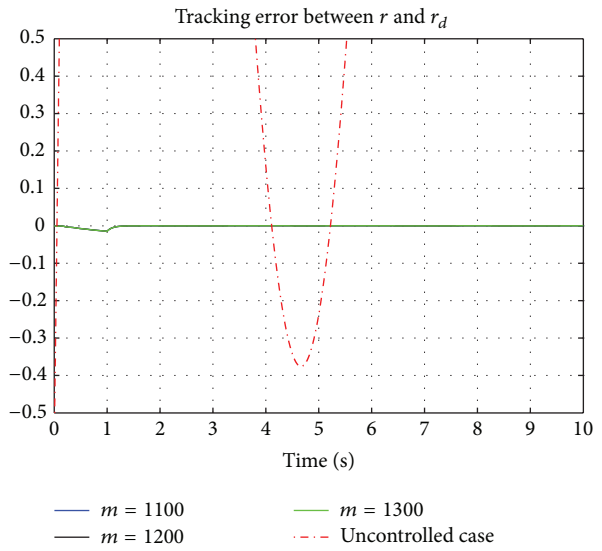

Figure 8: The local enlargement of Figure 7.

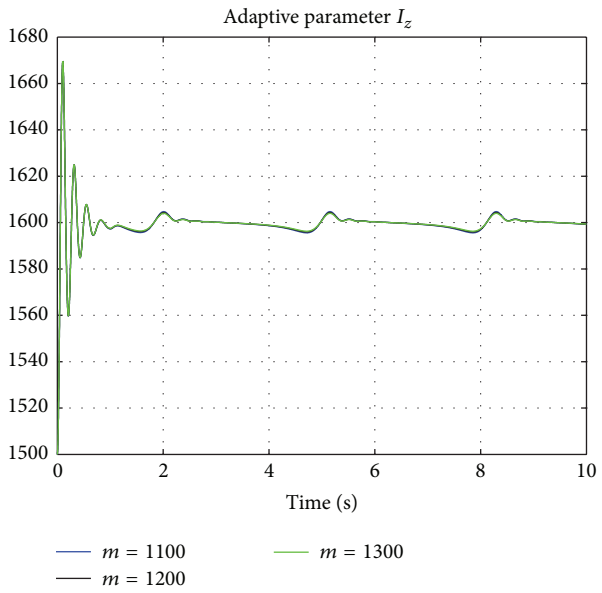

Figure 9: The moment of inertia about the yaw axis, I_z.

The simulation result in Figure 9 characterizes the adaptation of the uncertain parameter I_z, and from this figure we can see that the moment of inertia about the yaw axis I_z does converge to the true value (1600 kgm^2), which achieves the estimation of the uncertain parameters.

The control inputs (the yaw moment, M_z) for different cases are plotted in Figure 10.

4.2. Abrupt Demand Signal. Abrupt demand signal can be generally assumed as discrete events of relatively short duration and high intensity, and the corresponding function is given by

$$\delta = \begin{cases} \sin(t), & 1 \le t \le 1.25, \\ 0, & \text{otherwise.} \end{cases} \tag{74}$$

Bearing an analogy with the periodic input, the sideslip angle responses of the open-loop system, closed-loop systems with designed ARC controller for different vehicle masses are plotted in Figure 11. From Figure 11, we can see that the maximal response peak is less than 0.1 m by using the proposed controller, which has been reduced substantially compared with the open-loop system without controller

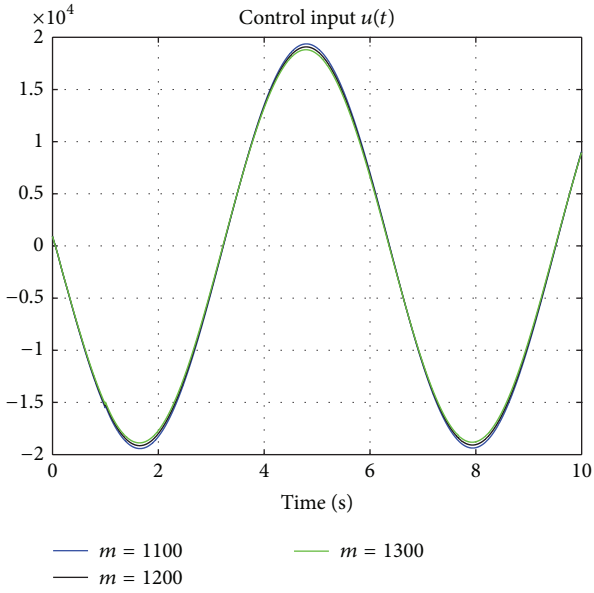

Figure 10: Control inputs, M_z.

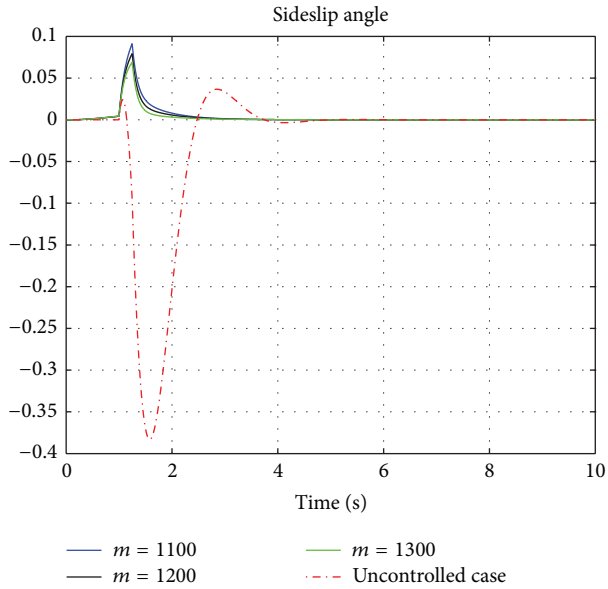

Figure 11: The sideslip angle responses of the open-loop system, closed-loop systems with designed ARC controller for different vehicle masses.

(the maximal response peak of open-loop systems is nearly 0.4 m). The proposed controller is also robust against the changing vehicle masses, which can be seen from Figures 11–14.

The time histories of yaw rate for both open-loop systems and closed-loop systems with ARC controller in the case of different vehicle masses are shown in Figure 12, and Figure 13 is the corresponding responses of tracking errors between the real yaw rate and the desired yaw rate. From these figures, we can see that the proposed controller yields the least value of the maximum tracking error, compared with the open-loop

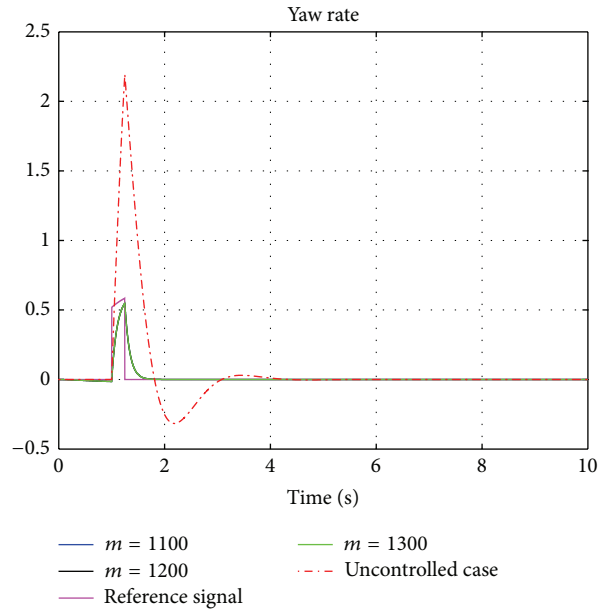

Figure 12: The yaw rate responses of the open-loop system, closed-loop systems with designed ARC controller for different vehicle masses.

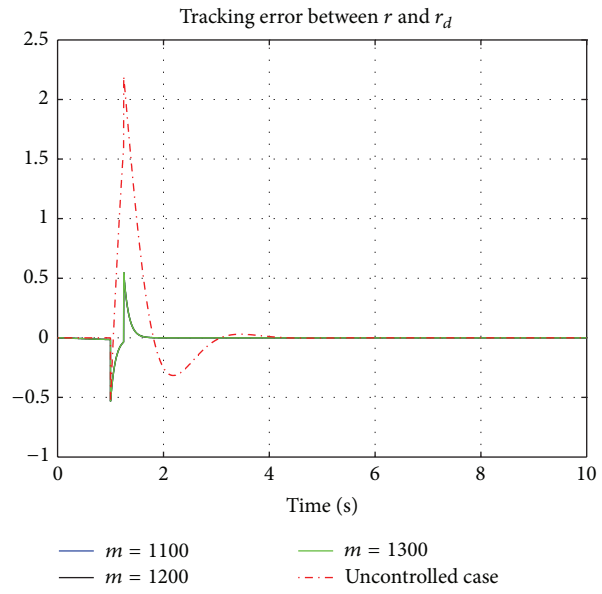

Figure 13: The tracking errors between real yaw rate and desired yaw rate of the open-loop system, closed-loop systems with designed ARC controller for different vehicle masses.

system. Figure 14 shows the yaw moment, M_z, for different cases (changing masses).

5. Concluding Remarks

In this paper, an adaptive robust control strategy has been proposed for vehicle lateral dynamic systems to improve vehicle handling and stability, where parameter uncertainties and external nonlinearities are considered in a unified

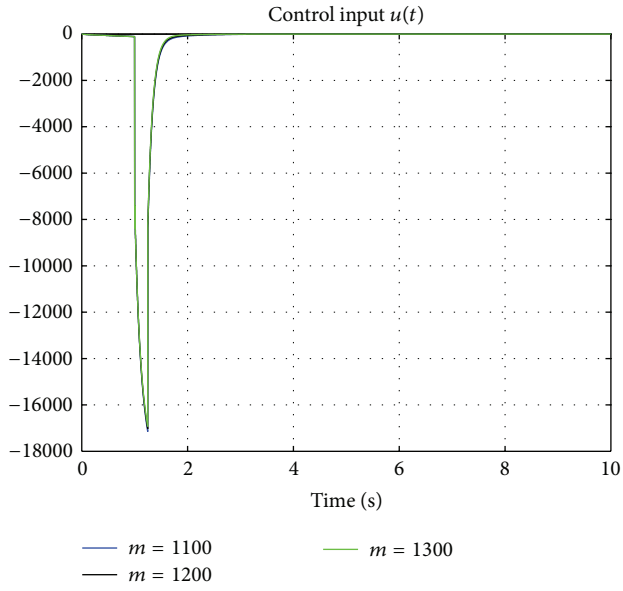

Figure 14: Control inputs, M_z.

framework. In order to manage two conflicting indexes, a compromise of the requirements is made, and the desired sideslip angle is replanned as a new reference signal, instead of the ideal "zero." To the end, the designed controller can not only accomplish the required control purposes, but also effectively attenuate both the changes of vehicle mass and the variations of cornering stiffness. In addition, to overcome the problem of "explosion of complexity" caused by backstepping method in the traditional ARC design, the dynamic surface control (DSC) technique has been used to estimate the derivative of the virtual control. Finally, a nonlinear vehicle model is employed as the design example to illustrate the effectiveness of the proposed control law.

Conflict of Interests

The authors declare that there is no conflict of interests regarding the publication of this paper.

Acknowledgment

This work was supported in part by the self-planned task (no. SKLRS201308B) of the State Key Laboratory of Robotics and System (HIT), the Fundamental Research Funds for the Central Universities (no. HIT.NSRIF.2015032), China.

References

[1] A. R. W. Huang and C. Chen, "A low-cost driving simulator for full vehicle dynamics simulation," *IEEE Transactions on Vehicular Technology*, vol. 52, no. 1, pp. 162–172, 2003.

[2] L. Cai, A. B. Rad, and W.-L. Chan, "An intelligent longitudinal controller for application in semiautonomous vehicles," *IEEE Transactions on Industrial Electronics*, vol. 57, no. 4, pp. 1487–1497, 2010.

[3] D. Cao, X. Song, and M. Ahmadian, "Editors' perspectives: road vehicle suspension design, dynamics, and control," *Vehicle System Dynamics*, vol. 49, no. 1-2, pp. 3–28, 2011.

[4] F. U. Rehman and M. M. Ahmed, "Steering control algorithm for a class of wheeled mobile robots," *IET Control Theory and Applications*, vol. 1, no. 4, pp. 915–924, 2007.

[5] H. Xiao, W. Chen, H. Zhou, and J. W. Zu, "Integrated control of active suspension system and electronic stability programme using hierarchical control strategy: theory and experiment," *Vehicle System Dynamics*, vol. 49, no. 1-2, pp. 381–397, 2011.

[6] H. Chou and B. D'Andréa-Novel, "Global vehicle control using differential braking torques and active suspension forces," *Vehicle System Dynamics*, vol. 43, no. 4, pp. 261–284, 2005.

[7] J.-H. She, X. Xin, and Y. Ohyama, "Estimation of equivalent input disturbance improves vehicular steering control," *IEEE Transactions on Vehicular Technology*, vol. 56, no. 6, pp. 3722–3731, 2007.

[8] J. Song and W. S. Che, "Comparison between braking and steering yaw moment controllers considering ABS control aspects," *Mechatronics*, vol. 19, no. 7, pp. 1126–1133, 2009.

[9] M. Bertoluzzo and G. Buja, "Development of electric propulsion systems for light electric vehicles," *IEEE Transactions on Industrial Informatics*, vol. 7, no. 3, pp. 428–435, 2011.

[10] P. Falcone, F. Borrelli, J. Asgari, H. E. Tseng, and D. Hrovat, "Predictive active steering control for autonomous vehicle systems," *IEEE Transactions on Control Systems Technology*, vol. 15, no. 3, pp. 566–580, 2007.

[11] S. Han and K. Huh, "Monitoring system design for lateral vehicle motion," *IEEE Transactions on Vehicular Technology*, vol. 60, no. 4, pp. 1394–1403, 2011.

[12] W. Cho, J. Yoon, J. Kim, J. Hur, and K. Yi, "An investigation into unified chassis control scheme for optimised vehicle stability and manoeuvrability," *Vehicle System Dynamics*, vol. 46, no. 1, pp. 87–105, 2008.

[13] C. March and T. Shim, "Integrated control of suspension and front steering to enhance vehicle handling," *Journal of Automobile Engineering: Proceedings of the Institution of Mechanical Engineers Part D*, vol. 221, no. 4, pp. 377–391, 2007.

[14] S.-B. Lu, Y.-N. Li, S.-B. Choi, L. Zheng, and M.-S. Seong, "Integrated control on MR vehicle suspension system associated with braking and steering control," *Vehicle System Dynamics*, vol. 49, no. 1-2, pp. 361–380, 2011.

[15] Q. Zhou, P. Shi, J. Lu, and S. Xu, "Adaptive output-feedback fuzzy tracking control for a class of nonlinear systems," *IEEE Transactions on Fuzzy Systems*, vol. 19, no. 5, pp. 972–982, 2011.

[16] H. Du, N. Zhang, and G. Dong, "Stabilizing vehicle lateral dynamics with considerations of parameter uncertainties and control saturation through robust yaw control," *IEEE Transactions on Vehicular Technology*, vol. 59, no. 5, pp. 2593–2597, 2010.

[17] E. Gartley and D. M. Bevly, "Online estimation of implement dynamics for adaptive steering control of farm tractors," *IEEE/ASME Transactions on Mechatronics*, vol. 13, no. 4, pp. 429–440, 2008.

[18] H. Lee and M. Tomizuka, "Adaptive vehicle traction force control for Intelligent Vehicle Highway Systems (IVHSs)," *IEEE Transactions on Industrial Electronics*, vol. 50, no. 1, pp. 37–47, 2003.

[19] J. Ahmadi, A. K. Sedigh, and M. Kabganian, "Adaptive vehicle lateral-plane motion control using optimal tire friction forces with saturation limits consideration," *IEEE Transactions on Vehicular Technology*, vol. 58, no. 8, pp. 4098–4107, 2009.

[20] N. Ding and S. Taheri, "An adaptive integrated algorithm for active front steering and direct yaw moment control based on direct Lyapunov method," *Vehicle System Dynamics*, vol. 48, no. 10, pp. 1193–1213, 2010.

[21] L. Xu and H. E. Tseng, "Robust model-based fault detection for a roll stability control system," *IEEE Transactions on Control Systems Technology*, vol. 15, no. 3, pp. 519–528, 2007.

[22] Z. He and X. Ji, "Nonlinear robust control of integrated vehicle dynamics," *Vehicle System Dynamics*, vol. 50, no. 2, pp. 247–280, 2012.

[23] H. Karimi, M. Zapateiro, and N. Luo, "An LMI approach to H_∞ control of vehicle engine-body vibration systems with time-varying actuator delay," *Journal of Systems and Control Engineering: Proceedings of the Institution of Mechanical Engineers Part I*, vol. 222, no. 8, pp. 883–899, 2008.

[24] H. Li, X. Jing, and H. Karimi, "Output-feedback based H_∞ control for active suspension systems with control delay," *IEEE Transactions on Industrial Electronics*, vol. 61, no. 1, pp. 436–446, 2014.

[25] W. Sun, Y. Zhao, J. Li, L. Zhang, and H. Gao, "Active suspension control with frequency band constraints and actuator input delay," *IEEE Transactions on Industrial Electronics*, vol. 59, no. 1, pp. 530–537, 2012.

[26] Z. Wang, Y. Liu, and X. Liu, "H_∞ filtering for uncertain stochastic time-delay systems with sector-bounded nonlinearities," *Automatica*, vol. 44, no. 5, pp. 1268–1277, 2008.

[27] H. R. Karimi, "Optimal vibration control of vehicle engine-body system using Haar functions," *International Journal of Control, Automation and Systems*, vol. 4, no. 6, pp. 714–724, 2006.

[28] H. Li, H. Liu, H. Gao, and P. Shi, "Reliable fuzzy control for active suspension systems with actuator delay and fault," *IEEE Transactions on Fuzzy Systems*, vol. 20, no. 2, pp. 342–357, 2012.

[29] J. Cao, P. Li, and H. Liu, "An interval fuzzy controller for vehicle active suspension systems," *IEEE Transactions on Intelligent Transportation Systems*, vol. 11, no. 4, pp. 885–895, 2010.

[30] H. Li, J. Yu, C. Hilton, and H. Liu, "Adaptive sliding mode control for nonlinear active suspension vehicle systems using T-S fuzzy approach," *IEEE Transactions on Industrial Electronics*, vol. 60, no. 8, pp. 3328–3338, 2013.

[31] O. Kaynak and A. Denker, "Discrete-time sliding mode control in the presence of system uncertainty," *International Journal of Control*, vol. 57, no. 5, pp. 1177–1189, 1993.

[32] X. Yu, M. O. Efe, and O. Kaynak, "A general backpropagation algorithm for feedforward neural networks learning," *IEEE Transactions on Neural Networks*, vol. 13, no. 1, pp. 251–254, 2002.

[33] Y. Tang, H. Gao, W. Zou, and J. Kurths, "Distributed synchronization in networks of agent systems with nonlinearities and random switchings," *IEEE Transactions on Cybernetics*, vol. 43, no. 1, pp. 358–370, 2013.

[34] Y. Tang and W. Wong, "Distributed synchronization of coupled neural networks via randomly occurring control," *IEEE Transactions on Neural Networks and Learning Systems*, vol. 24, no. 3, pp. 435–447, 2013.

[35] Q. Zhou, P. Shi, H. Liu, and S. Xu, "Neural network based decentralized adaptive output-feedback control for large-scale stochastic nonlinear systems," *IEEE Transactions on Systems, Man, and Cybernetics B*, vol. 42, no. 6, pp. 1608–1619, 2012.

[36] Q. Zhou, P. Shi, S. Xu, and H. Li, "Observer-based adaptive neural network control for nonlinear stochastic systems with time-delay," *IEEE Transactions on Neural Networks and Learning Systems*, vol. 24, no. 1, pp. 71–80, 2013.

[37] M. Zapateiro, N. Luo, H. R. Karimi, and J. Vehí, "Vibration control of a class of semiactive suspension system using neural network and backstepping techniques," *Mechanical Systems and Signal Processing*, vol. 23, no. 6, pp. 1946–1953, 2009.

[38] M. Zapateiro, F. Pozo, H. R. Karimi, and N. Luo, "Semiactive control methodologies for suspension control with magnetorheological dampers," *IEEE/ASME Transactions on Mechatronics*, vol. 17, no. 2, pp. 370–380, 2012.

[39] L. Zuo, J.-J. E. Slotine, and S. A. Nayfeh, "Model reaching adaptive control for vibration isolation," *IEEE Transactions on Control Systems Technology*, vol. 13, no. 4, pp. 611–617, 2005.

[40] S. Yin, H. Luo, and S. Ding, "Real-time implementation of fault-tolerant control systems with performance optimization," *IEEE Transactions on Industrial Electronics*, vol. 61, no. 5, pp. 2402–2411, 2014.

[41] S. Yin, S. Ding, A. Haghani, H. Hao, and P. Zhang, "A comparison study of basic data-driven fault diagnosis and process monitoring methods on the benchmark Tennessee Eastman process," *Journal of Process Control*, vol. 22, no. 9, pp. 1567–1581, 2012.

[42] B. Yao, F. Bu, J. Reedy, and G. T.-C. Chiu, "Adaptive robust motion control of single-rod hydraulic actuators: theory and experiments," *IEEE/ASME Transactions on Mechatronics*, vol. 5, no. 1, pp. 79–91, 2000.

[43] J. Yao, Z. Jiao, and D. Ma, "Adaptive robust control of DC motors with extended state observer," *IEEE Transactions on Industrial Electronics*, vol. 61, no. 7, pp. 3630–3637, 2014.

[44] J. Yao, Z. Jiao, D. Ma, and L. Yan, "High-accuracy tracking control of hydraulic rotary actuators with modeling uncertainties," *IEEE/ASME Transactions on Mechatronics*, no. 99, pp. 1–9, 2013.

[45] H. Liu, "Exploring human hand capabilities into embedded multifingered object manipulation," *IEEE Transactions on Industrial Informatics*, vol. 7, no. 3, pp. 389–398, 2011.